



Potential energy landscape signatures of slow dynamics in glass forming liquids

Srikanth Sastry^{a,*}, Pablo G. Debenedetti^b, Frank H. Stillinger^c,
Thomas B. Schröder^{d,e}, Jeppe C. Dyre^e, Sharon C. Glotzer^{d,f}

^aJawaharlal Nehru Centre for Advanced Scientific Research Jakkur Campus, Bangalore 560064, India

^bDepartment of Chemical Engineering, Princeton University, Princeton, NJ 08544, USA

^cBell Laboratories, Lucent Technologies, Murray Hill, NJ 07974, USA,

and Princeton Materials Institute, Princeton University, Princeton, NJ 08544, USA

^dCenter for Theoretical and Computational Materials Science, National Institute of Standards and Technology, Gaithersburg, MD 20899, USA

^eDepartment of Mathematics and Physics (IMFUFA), Roskilde University, P.O. Box 260, DK-4000 Roskilde, Denmark

^fPolymers Division, National Institute of Standards and Technology, Gaithersburg, MD 20899, USA

Abstract

We study the properties of local potential energy minima ('inherent structures') sampled by liquids at low temperatures as an approach to elucidating the mechanisms of the observed dynamical slowing down observed as the glass transition temperature is approached. This onset of slow dynamics is accompanied by the sampling of progressively deeper potential energy minima. Further, evidence is found in support of a qualitative change in the inherent structures sampled in a temperature range that includes the mode coupling critical temperature T_c , such that a separation of vibrational relaxation within inherent structure basins from that due to inter-basin transitions becomes valid at temperatures $T < T_c$. Average inherent structure energies do not show any qualitatively significant system size dependence. © 1999 Published by Elsevier Science B.V. All rights reserved.

Most liquids, when cooled to low temperatures under equilibrium conditions, freeze at a well-defined temperature to form a crystalline solid. It is often possible to cool a liquid below its freezing temperature without an alteration of state, and thereby study properties of the liquid under metastable, 'supercooled', conditions. Though supercooled liquids eventually attain the lower free energy solid state through the processes of homogeneous or heterogeneous nucleation, it is possible to maintain the supercooled liquid state over wide ranges of temperatures for long intervals of time. Such liquids,

* Corresponding author.

upon progressive lowering of the temperature below the freezing temperature, display strong temperature dependence of their relaxation properties, such that they no longer equilibrate below a finite temperature, which depends on the rate at which the liquid is cooled and the experimental probes employed to determine equilibration. This ‘falling out of equilibrium’ at a finite temperature constitutes the laboratory glass transition [1]. A detailed understanding of the strong, apparently divergent, temperature dependence of relaxation properties and their possible origin in a thermodynamic, ideal, glass transition is at present incomplete, and forms the motivation of the present work.

The approach we consider is the characterization of the configuration space explored by the system in terms of the potential energy minima to which instantaneous configurations of the liquid map under a local minimization of the potential energy. The properties of such local minima, termed inherent structures [2], have been studied by many workers as a useful approach to understanding glassy behavior [3–17]. Particular issues addressed are the relationship between the distribution of inherent structures as a function of their energy and the thermodynamic transition that may underlie glassy behavior [4,7,9–11], the role of transitions between inherent structure basins in the system’s dynamics [5,6,12,14–17], and structural change upon lowering temperature [8]. Similar studies have also been conducted to analyze local ‘free energy’ minima for the hard sphere system [18]. Here, we discuss results concerning the onset of ‘slow dynamics’ (the onset of stretched exponential relaxation and deviation from the Arrhenius temperature dependence of relaxation times) and the transition to a temperature regime wherein relaxation has been proposed to be dictated by activated transitions between potential energy minima across significant energy barriers. The results are obtained from computer simulations of two model liquids. Each is a binary mixture of atomic species, interacting via the Lennard–Jones potential. The first model liquid (referred to henceforth as the ‘80:20 binary mixture’) consists of 80% of particles of type A and 20% of particles of type B, with Lennard–Jones parameters $\epsilon_{AA} = 1.0$, $\epsilon_{AB} = 1.5$, $\epsilon_{BB} = 0.5$, $\sigma_{AA} = 1.0$, $\sigma_{AB} = 0.8$, and $\sigma_{BB} = 0.88$, and a ratio of masses $m_B/m_A = 1$. The second model liquid (referred to as the ‘50:50 binary mixture’) consists of 50% each of particles of type A and B, with parameters $\sigma_{BB}/\sigma_{AA} = 5/6$, $\sigma_{AB} = (\sigma_{AA} + \sigma_{BB})/2$, and $\epsilon_{AA} = \epsilon_{AB} = \epsilon_{BB}$, and a ratio of masses $m_B/m_A = 1/2$. In each case, molecular dynamics simulations are performed at a series of temperatures, at reduced density $\rho = 1.2$ for the 80:20 binary mixture and at $\rho = 1.296$ for the 50:50 binary mixture. Inherent structures are generated by local minimization of the potential energy of selected instantaneous configurations. Further details have been presented elsewhere [14,16,17].

Fig. 1 shows the potential energies of inherent structures as a function of temperature for the 80:20 binary mixture, averaged over 100 configurations for sizes $N = 256, 1372$, over 20 configurations for $N = 10\,976$ and over 10 configurations for $N = 19\,652$. Even though the data shown display dependence on system size, the qualitative behavior is the same: For temperatures above $T = 1$, the energies are seen to approach a constant value, while at lower temperatures they display a clear temperature dependence. The saturation at higher temperatures is confirmed by calculations over a wider range of

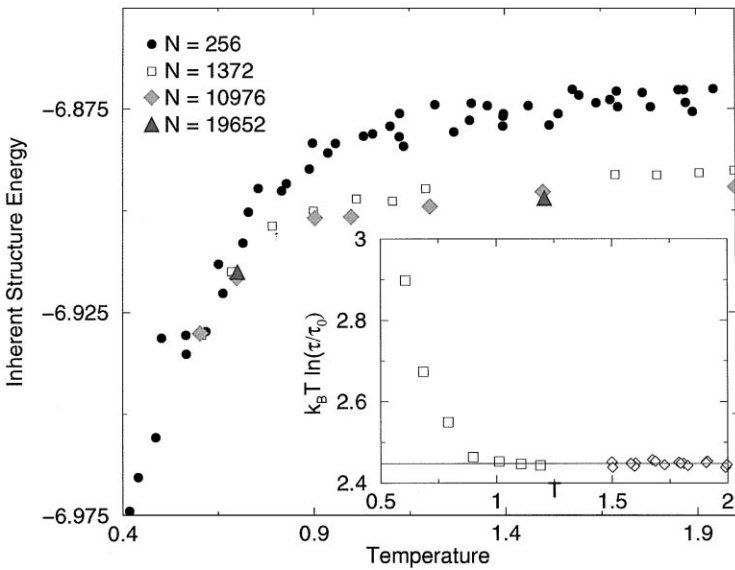


Fig. 1. Average inherent structure energies per particle for a range of temperatures for the 80:20 binary mixture, for system sizes $N = 256, 1372, 10976, 19652$. Inset shows transformed values of relaxation times plotted against temperature.

temperature values (data not shown). It is seen that the biggest change with system size occurs between $N = 256$ and 1372 , while the energies are not significantly altered for larger system sizes. A systematic study of the size dependence, however, remains to be performed. The comparison of the temperature dependence of inherent structure energies with the relaxation behavior of the system is performed by first calculating relaxation times from the self-intermediate scattering function $F_s(q, t)$ (Fourier transform of the van Hove self-correlation function $G_s(r, t)$ which describes the probability of finding a particle a distance r away at time t from its position at time $t = 0$; the wave vector magnitude q is chosen to be close to the first peak of the structure factor). These relaxation times $\tau(T)$ are plotted, in the inset of Fig. 1, in such a manner that if they obey an Arrhenius dependence $\tau = \tau_0 \exp(E/k_B T)$, the plotted numbers are temperature independent. It is apparent from the inset of Fig. 1 that $\tau(T)$ departs from Arrhenius behavior below $T = 1$, in correspondence with the temperature behavior of the inherent structure energies. Fig. 2 shows the average inherent structure energies for the 50:50 binary mixture, which displays behavior similar to the 80:20 binary mixture. Shown in the inset of Fig. 2 is the temperature dependence of the stretching exponent β obtained from stretched exponential fits of $F_s(q, t)$, which also shows temperature dependence corresponding to that of the inherent structure energies, deviating from a high-temperature value of 1.0 to lower values at low temperatures. It must be noted that the temperature dependence of the inherent structure energies and correspondingly those of $\tau(T)$, $\beta(T)$ are gradual despite clearly identifiable qualitative changes from high to low temperatures.

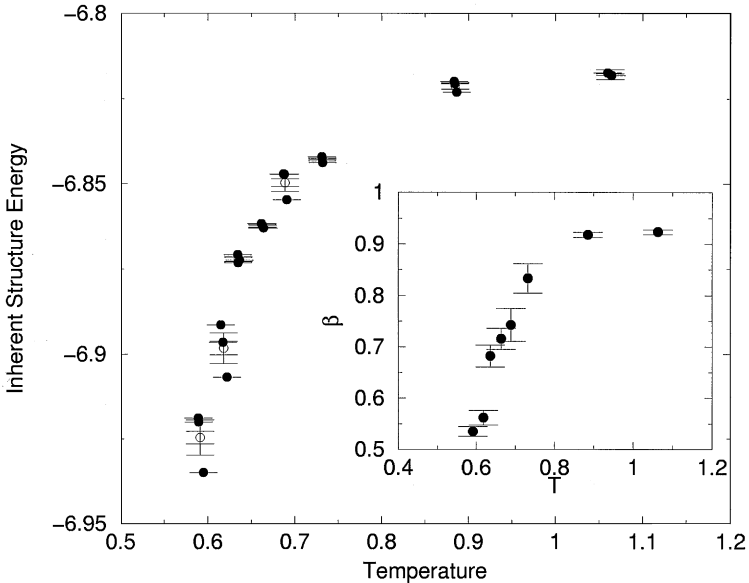


Fig. 2. Shows the average inherent structure energies per particle for a range of temperatures for the 50:50 binary mixture, for system size $N = 500$. Inset shows the stretching exponent β .

Based on power-law fits to the relaxation times and diffusion coefficients, the mode coupling critical temperature is estimated to be $T_c = 0.45$ for the 80:20 binary mixture and $T_c = 0.592$ for the 50:50 binary mixture. The power-law singularity in relaxation times as predicted by ideal mode coupling theory [19–21] is not in fact observed; it has been argued that this singularity is instead ‘rounded out’ due to single particle ‘hopping’ processes, unaccounted for in ideal mode coupling theory. It has been argued [6,22] that the mode coupling T_c coincides with a crossover temperature discussed earlier by Goldstein [5] below which activated energy barrier crossing becomes important for the relaxation of the system. A similar picture has also been discussed in the context of mean field theories of certain spin glass models [23–28].

Indeed, a qualitative change in the dynamics is observed near the estimated T_c value for both models considered here. Fig. 3 shows the van Hove self-correlation function $G_s(r, t)$ for the 50:50 binary mixture, where for each temperature, the time t is chosen such that the mean squared displacement $\langle r^2(t) \rangle = 1$. While at high temperatures a Gaussian form is a good approximation of $G_s(r, t)$, a progressive deviation from the Gaussian shape is seen going to low temperatures. At the two lowest temperatures, one has clearly identifiable secondary peaks, interpreted usually as indicating single-particle hopping [29,30].

In seeking evidence of the changes in the sampled potential energy landscape, we first note that the average inherent structures energies show no clear change in the relevant temperature range. There are, however, signatures to be found in the topography of potential energy basins, and in transitions between basins, as we now discuss.

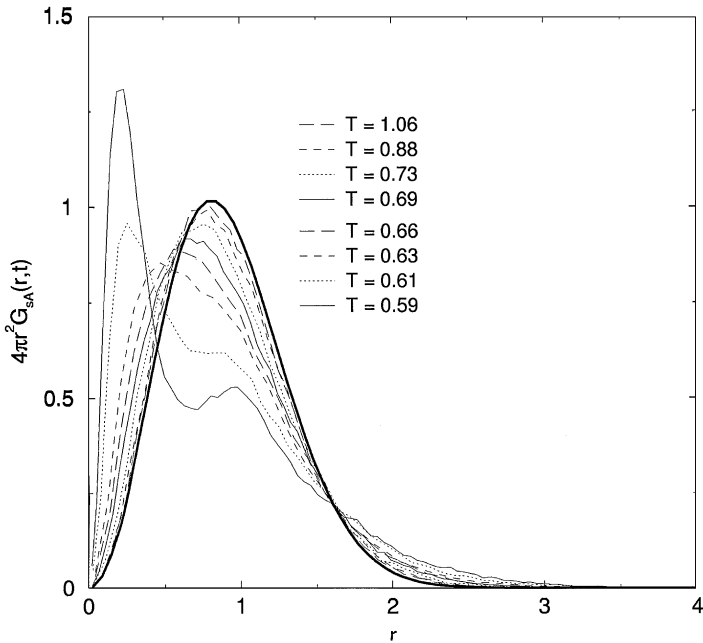


Fig. 3. Distribution of particle displacements, for the A particles in the 50:50 binary mixture, $4\pi r^2 G_{sA}(r, t_1)$, where t_1 is defined by $\langle r^2(t_1) \rangle_A = 1$. At high T the Gaussian approximation (thick curve) is reasonable, whereas at the lowest T a second peak is present, indicating single particle hopping.

It has been shown in Ref. [14] that the mean squared distance between instantaneous configurations and the corresponding inherent structures displays a deviation from linearity (the expected behavior for a harmonic system) for temperatures above the estimated T_c for the 80:20 binary mixture. The mean squared distance is the Euclidean distance in configuration space between the location of an instantaneous configuration $\mathbf{R}(t)$ and the corresponding inherent structure configuration $\mathbf{R}^I(t)$. Alternately, one can consider the ‘path length’ travelled by the system in the course of finding the local energy minimum starting from an instantaneous configuration, which provides information about the ‘ruggedness’ of the potential energy basins. Fig. 4 shows the temperature dependence of the path length for the 80:20 binary mixture for a cooling rate (see Ref. [14] for details) of 8.33×10^{-5} . The path length displays a marked increase above $T = 0.5$, compared to extrapolated values from lower temperatures, indicating that the potential energy basins become more rugged at higher temperatures. To demonstrate that this increase is not simply a result of an increase in mean squared distance from the inherent structures, the inset of Fig. 4 shows the dependence of the path length on the root mean squared distance. Again, it is observed that the path lengths at temperatures above $T = 0.5$ show deviation towards higher values when compared to the low-temperature behavior. A related analysis in the case of supercooled water also lead similar conclusions [12].

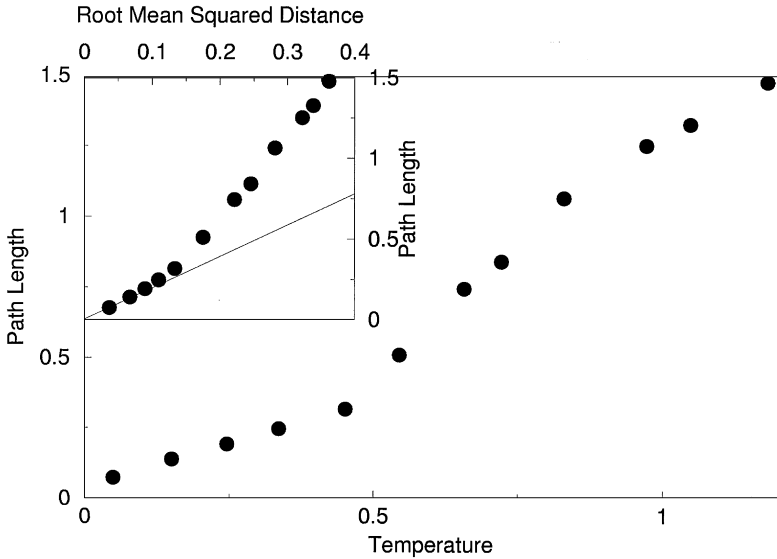


Fig. 4. The length of the path taken by the system during potential energy minimization, from the instantaneous configuration to the inherent structure, showing marked deviation from low-temperature behavior above $T = 0.5$. The inset shows the dependence of the path length on the root mean squared distance between instantaneous and inherent structures. This confirms that the excess increase in the path length at $T > 0.5$ is not simply due to an increase in the Euclidean distance between instantaneous and inherent structure configurations. The straight line in the inset is drawn to guide the eye.

A more direct analysis of the changes occurring near T_c is accomplished by considering a mapping of the dynamics of the system to the dynamics described by the time series of inherent structures to which instantaneous configurations map [16,17]. Fig. 5(a) shows $F_{sA}(q, t)$ for the true trajectory for a range of temperatures, along with stretched exponential fits for the long time dynamics. These curves show the development of two step relaxation at low temperatures, where the short time, fast decay is associated with ‘vibrational’ relaxation (see, e.g. [12]). When the system experiences significant energy barriers between potential energy minima, argued to occur as one cools the system below mode coupling T_c [5,6,22], one expects a clear separation between the short time vibrational relaxation and the long time relaxation due to transitions between inherent structure basins. This would mean that the dynamics as reflected by the inherent structures (which suppress all motion within each inherent structure basin) show no short time relaxation. Data shown in Fig. 5(b) of the self-intermediate scattering functions for the time series of inherent structures, $F_{sA}^I(q, t)$, show that this expectation becomes fulfilled as one approaches T_c , while at higher temperatures, no clear separation between intra- and inter-basin relaxations is present. Figs. 5(c) and (d) show the pre-factor in the stretched exponential fits (the ‘non-ergodicity factor’) to the long time behavior of $F_{sA}(q, t)$ and $F_{sA}^I(q, t)$, respectively. The approach of the non-ergodicity parameter f_c^I to the value 1 as $T \rightarrow T_c$ quantitatively demonstrates the

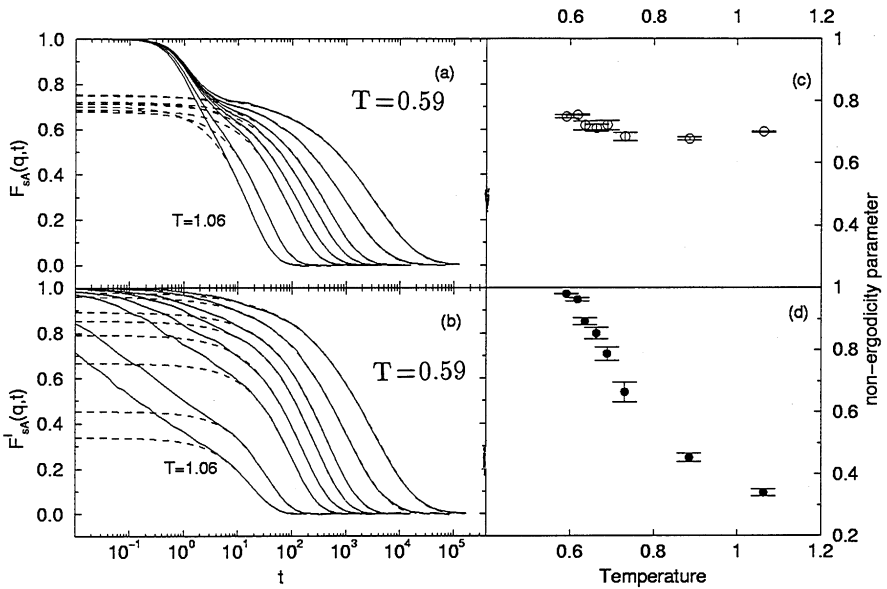


Fig. 5. Self intermediate scattering functions for A particles, 50:50 binary mixture. (a) $F_{SA}(q, t)$ plotted versus $\ln t$ for $q = 7.5$. The dashed lines are fits to $f(t) = f_c \exp(-(t/\tau_x)^\beta)$. (b) $F_{SA}^I(q, t)$ plotted versus $\ln t$ for $q = 7.5$. The dashed lines are fits to $f(t) = f_c^I \exp(-(t/\tau_x^I)^\beta)$. In both (a) and (b), the fit was performed for $t > 30$ for $T \leq 0.73$ and $t > 10$ otherwise. The panels (c) and (d) show the non-ergodicity factors f_c , f_c^I for the true and inherent dynamics, respectively.

separation of intra- and inter-basin relaxations as $T \rightarrow T_C$, supporting thereby arguments previously presented [5,6,22].

In summary, analysis of the onset and qualitative changes of slow dynamics in model liquids above their glass transition temperatures has been performed, by studying the properties of local potential energy minima – inherent structures – sampled by the system at different temperatures, and transitions between inherent structures. We have presented evidence that shows clear correlation of the onset of slow dynamics with the probing by the system of progressively deeper potential energy minima, and evidence that directly supports the association of the mode coupling critical temperature T_c with a temperature regime where the crossing of significant energy barriers becomes the dominant mechanism of relaxation.

References

- [1] P.G. Debenedetti, *Metastable Liquids*, Princeton University Press, Princeton, 1996.
- [2] F.H. Stillinger, T.A. Weber, *Phys. Rev. A* 28 (1983) 2408.
- [3] F.H. Stillinger, *Science* 267 (1995) 1935.
- [4] C.A. Angell, *Science* 267 (1995) 1924.
- [5] M. Goldstein, *J. Chem. Phys.* 51 (1969) 3728.
- [6] C.A. Angell, *J. Phys. Chem. Sol.* 49 (1988) 863.
- [7] F.H. Stillinger, *J. Chem. Phys.* 88 (1988) 7818.
- [8] H. Jónsson, H.C. Andersen, *Phys. Rev. Lett.* 60 (1988) 2295.

- [9] R.J. Speedy, *J. Chem. Phys.* 100 (1994) 6684.
- [10] R.J. Speedy, P.G. Debenedetti, *Mol. Phys.* 88 (1996) 1293.
- [11] R.J. Speedy, *Mol. Phys.* 95 (1998) 169.
- [12] F. Sciortino, P. Tartaglia, *Phys. Rev. Lett.* 78 (1997) 2385.
- [13] A. Heuer, *Phys. Rev. Lett.* 78 (1997) 4051.
- [14] S. Sastry, P.G. Debenedetti, F.H. Stillinger, *Nature* 393 (1998) 554.
- [15] L. Angelani, G. Parisi, G. Ruocco, G. Vilianni, *Phys. Rev. Lett.* 81 (1998) 4648.
- [16] T.B. Schröder, S. Sastry, J.C. Dyre, S.C. Glotzer, *cond-mat/9901271*.
- [17] T.B. Schröder, J.C. Dyre, *J. Non-Cryst. Solids* 235–237 (1998) 331.
- [18] C. Dasgupta, O.T. Valls, *Phys. Rev. E* 53 (1996) 2603; *Phys. Rev. E* 59 (1999) 3123.
- [19] W. Götze, L. Sjögren, *Rep. Prog. Phys.* 55 (1992) 241.
- [20] U. Bengtzelius, W. Götze, A. Sjölander, *J. Phys. C* 17 (1984) 5915.
- [21] E. Leutheusser, *Dynamical Model for the Liquid–Glass Transition*, *Phys. Rev. A* 29 (1984) 2765.
- [22] A.P. Sokolov, *J. Non-Cryst. Solids* 235–237 (1988) 190.
- [23] T.R. Kirkpatrick, D. Thirumalai, *Phys. Rev. B* 36 (1987) 5388.
- [24] T.R. Kirkpatrick, P.G. Wolynes, *Phys. Rev. B* 36 (1987) 8552.
- [25] T.R. Kirkpatrick, D. Thirumalai, P.G. Wolynes, *Phys. Rev. A* 40 (1989) 1045.
- [26] A. Cavagna, I. Giardina, G. Parisi, *Phys. Rev. B* 57 (1998) 11251.
- [27] S. Franz, G. Parisi, *Phys. Rev. Lett.* 79 (1997) 2486.
- [28] M. Cardenas, S. Franz, G. Parisi, *J. Chem. Phys.* 110 (1999) 1726.
- [29] J.-N. Roux, J.-L. Barrat, J.-P. Hansen, *J. Phys.: Condens. Matter* 1 (1989) 7171.
- [30] G. Wahnström, *Phys. Rev. A* 44 (1991) 3752.